ELSEVIER

Non-isothermal kinetics of pyrolysis of rice husk

L.T. Vlaev[*], I.G. Markovska, L.A. Lyubchev

Department of Physical Chemistry, Assen Zlatarov University, 8010 Bourgas, Bulgaria

Abstract

The kinetics of pyrolysis of rice husk was studied under non-isothermal heating in air or nitrogen media. Based on TG curves, the kinetic parameters of the process were calculated using the method of Coats–Redfern and fourteen kinetic equations. It was found that the experimental data were best described by the equation of Ginstling–Brounshtein valid for diffusion-controlled reactions starting on the exterior of spherical particles with uniform radius. The values of activation energy, frequency factor, change of entropy, enthalpy and Gibbs energy were calculated for the formation of the active complex of the reagent. The diffusion control of the pyrolysis process was explained with the high strength of the Si–O carcass of the biomass which impeded the release of volatile products. It was confirmed also by the similarity of the kinetic curves and electron microscopy photographs of the hard residue obtained after pyrolysis in oxidative or inert medium.
© 2003 Elsevier B.V. All rights reserved.

Keywords: Non-isothermal kinetics; Rice husk; Pyrolysis; Thermogravimetric analysis

1. Introduction

Husk is a major by-product of the rice milling industry. Its utilization as a valuable product has always been a problem. It is well known that, among the various biomasses, rice husk is a potential source of energy [1] and value-added by-products [2,3]. Recently, the carbon-free ash (white ash) obtained from rice husk opened a new dimension in its utilization concept [4,5]. White ash, as a source of high grade amorphous silica can be used for production of silicon [5,6]. Besides, rice husk turned out to be a perspective and cheap raw material for production of Si, SiC, Si_3N_4, SiO_2 and other materials [7–9]. Investigations showed that the interest towards rice husk is increasing world-wide. It is connected with the leading role of rice as a grain culture from which waste products

can not be used as food, fertilizer or fuel. In this aspect, the problem with the utilization of the large amounts of this material elimination of certain ecological threat remains to be solved [10,11]. Various technologies for utilization of rice husk through biological and thermochemical conversion are being developed. The design of proper equipment for rice husk conversion requires sound knowledge of pyrolysis and gasification kinetics. However, few literature sources on these aspects are available. It is known [2,12,13] that the thermal decomposition of rice husk occurs in three main stages, namely, drying (40–150 °C), removal of organic volatile matters (215–350 °C) and combustion of carbon (350–690 °C).

Several kinetic models for pyrolysis of rice husk have been published [3,14–16]. Some of their authors have represented the pyrolysis reaction mainly by *n*th-order expressions. Depending on the conditions for thermal treatment, however, other kinetic equations such as nucleation and nucleus growing, phase

* Corresponding author.
E-mail address: vlaev@btu.bg (L.T. Vlaev).

boundary reactions, diffusion or power law can also be used to describe the different stages of the process [16,17].

The aim of the present work is to find the values of the kinetic parameters characterizing the pyrolysis of rice husk in oxidative or inert medium using data from non-isothermal thermogravimetry and the calculation procedure of Coats and Redfern.

2. Experimental

The experiments under non-isothermal conditions were carried out in a derivatograph system F. Paulik–I. Paulik–L. Erdey (Hungary). Rice husk samples of 100 mg were used for the experiments. The TG, DTA and DTG curves were recorded graphically with 1 mg sensitivity. Alumina was used as a standard reference material. The content of SiO_2 in the solid residue was determined gravimetrically after treatment with hydrofluoric acid and the content of carbon—by automatic analyzer Carlo Erba, model 1104. The SEM analyses were performed on a scanning electron microscope Tesla BS 340 under regime of secondary electrons at acceleration of 20 kV. The samples were metallized with aluminium in Edwards 306 vacuum camera. The average thickness of the coating was measured to be 200 Å.

2.1. Materials and measurements

The rice husk was locally available material and had the following approximate dimensions: 8–10 mm long, 2.0–2.5 mm wide and 0.10–0.15 mm thick. The samples were heated to 1000 °C at heating rate of 10 °C/min by the following three methods:

- In static air, in the course of the heating, first the physically adsorbed water was released (5%), then pyrolysis takes place to form a hard residue (26%) containing 91.53% SiO_2.
- Carbonization of raw rice husk in nitrogen medium with flow rate 2.5 cm^3 min^{-1} at 20 °C and 1 atm pressure. Again physically adsorbed water was first released and the following pyrolysis of the organic mass gave hard residue (43%).
- The husk carbonized by the second method were further treated in static air medium. Thus, the carbon

mass was burned and the residue (51%) was hard SiO_2 containing negligible amount of carbon.

In further discussion the solid residues obtained by these three methods are referred to as A, B and C, respectively.

2.2. Theoretical background

Data from TG and DTG curves were used to determine the kinetic parameters. Mathematical analysis was performed by the integral method of Coats and Redfern [18,19]. This method has been successfully used for studies on the kinetics of decomposition of solid substances [20–24]. The data on decomposition reactions were analyzed by applying 14 kinetic models including processes governed by nuclei growth, surface nucleation followed by movement of the resulting surface, transport (diffusion) phenomena and chemical reactions [24–26].

The pyrolysis process may be represented by the following reaction scheme:

Biomass → solid residue + volatiles
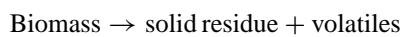
The kinetic equation of common type can be written as follows:

$$\frac{d\alpha}{d\tau} = k(T) f(\alpha) \tag{1}$$

where $f(\alpha)$ is a function, the type of which depends on the reaction mechanism, $k(T)$ the temperature dependent rate constant; T the absolute temperature, τ the time and α the degree of transformation. The temperature dependence of the rate constant usually described by the Arrhenius equation:

$$k = A \exp\left(-\frac{E}{RT}\right) \tag{2}$$

where A is pre-exponential or frequency factor, E the activation energy, R the universal gas constant (8.314 J mol^{-1} K^{-1}). Under constant heating rate:

$$\frac{dT}{d\tau} = q = \text{constant} \tag{3}$$

and after substitution in (1) and some transformations:

$$\int_0^\alpha \frac{d\alpha}{f(\alpha)} = \frac{A}{q} \int_0^T \exp\left(-\frac{E}{RT}\right) dT \tag{4}$$

The right hand side of Eq. (4) has no exact analytical solution, but making some variable substitutions and applying Cauchy's rule the expression can be solved to give:

$$\frac{A}{q}\int_0^T \exp\left(-\frac{E}{RT}\right)\mathrm{d}T$$
$$\cong \frac{ART^2}{qE}\left(1 - \frac{2RT}{E}\right)\exp\left(-\frac{E}{RT}\right) \tag{5}$$

If the solution of the integral on the left-hand-side of Eq. (4) is denoted with:

$$g(\alpha) = \int_0^\alpha \frac{\mathrm{d}\alpha}{f(\alpha)} \tag{6}$$

then, after division by T^2 taking logarithms, Eq. (4) is transformed to:

$$\ln\frac{g(\alpha)}{T^2} = \ln\frac{AR}{qE}\left(1 - \frac{2RT}{E}\right) - \frac{E}{RT} \tag{7}$$

Since $2RT/E \ll 1$,

$$\ln\frac{g(\alpha)}{T^2} = \ln\frac{AR}{qE} - \frac{E}{RT} \tag{8}$$

Thus, a plot of $\ln[g(\alpha)/T^2]$ against $1/T$ should be a straight line with a slope $-E/R$ since $\ln(AR/qE)$ is nearly constant.

The formal expressions of the functions $f(\alpha)$ and $g(\alpha)$ depend on the conversion mechanism and its mathematical model. The latter usually represents the limiting stage of the reaction—the chemical reaction; random nucleation and nuclei growth; phase boundary reaction or diffusion. If the correct $g(\alpha)$ is used, the plot of $\ln[g(\alpha)/T^2]$ against $1/T$ should give a straight line with high correlation coefficient of the linear regression analysis, from which the values of E and A can be derived. Table 1 shows the most common kinetic models and their algebraic expressions [24–26].

Here, α is the fractional pyrolysis of the biomass used, which is calculated from the corresponding TG curve by the formula:

$$\alpha = \frac{W_i - W_\tau}{W_i - W_f} \tag{9}$$

where W_i, W_τ and W_f are the initial, actual and final weight of the sample, respectively.

The other kinetic parameters of the process can be calculated using the fundamental equation of the theory of the active complex (preceding state)

Table 1
Algebraic expressions of functions of the most common reaction mechanisms operating in solid state reactions [24–26]

Mechanism	Symbol	$f(\alpha)$	$g(\alpha)$
Chemical reaction			
First-order	F1	$1 - \alpha$	$-\ln(1 - \alpha)$
Second-order	F2	$(1 - \alpha)^2$	$(1 - \alpha)^{-1} - 1$
Third-order	F3	$(1 - \alpha)^3$	$[(1-\alpha)^{-2} - 1]/2$
nth-order	Fn	$(1 - \alpha)^n$	$[(1 - \alpha)^{1-n} - 1]/n - 1$
Random nucleation and nuclei growth			
Bi-dimensional	A2	$2(1 - \alpha)[-\ln(1 - \alpha)]^{1/2}$	$[-\ln(1 - \alpha)]^{1/2}$
Tree-dimensional	A3	$3(1 - \alpha)[-\ln(1 - \alpha)]^{2/3}$	$[-\ln(1 - \alpha)]^{1/3}$
Limiting surface reaction between both phases			
One dimension	R1	1	α
Two dimensions	R2	$2(1 - \alpha)^{1/2}$	$1 - (1 - \alpha)^{1/2}$
Three dimensions	R3	$3(1 - \alpha)^{2/3}$	$1 - (1 - \alpha)^{1/3}$
Diffusion			
One-way transport	D1	$1/2\alpha$	α^2
Two-way transport	D2	$[-\ln(1 - \alpha)]^{-1}$	$\alpha + (1 - \alpha)\ln(1 - \alpha)$
Three-way transport	D3	$(2/3)(1 - \alpha)^{2/3}/1 - (1 - \alpha)^{1/3}$	$[1 - (1 - \alpha)^{1/3}]^2$
Ginstling–Brounshtein equation	G–B	$(2/3)(1 - \alpha)^{1/3}/1 - (1 - \alpha)^{1/3}$	$1 - 2\alpha/3 - (1 - \alpha)^{2/3}$
Zhuravlev equation	Zh	$(2/3)(1 - \alpha)^{5/3}/1 - (1 - \alpha)^{1/3}$	$[(1 - \alpha)^{-1/3} - 1]^2$

Table 2
Kinetic characteristics of rice husk pyrolysis

Parameters	Samples					
	A		B		C	
	$T < T_p$	$T > T_p$	$T < T_p$	$T > T_p$	$T < T_p$	$T > T_p$
$T_{p(exp)}$ (K)	593		633		853	
$T_{p(calc)}$ (K)	597		634		855	
R^2	0.9899	0.9950	0.9988	0.9822	0.9852	0.9947
E (kJ mol^{-1})	187.1	23.1	175.1	5.3	228.3	54.8
A (min^{-1})	3.45×10^{14}	2×10^{-1}	1.78×10^{13}	5.6×10^{-3}	6.49×10^{11}	3.89
k (min^{-1})	1.14×10^{-2}	1.85×10^{-3}	6.32×10^{-2}	$2.05.10^{-3}$	6.78×10^{-3}	1.17×10^{-3}
$-\Delta S^{\neq}$ (J mol^{-1} K^{-1})	14.7	306.4	39.9	336.6	69.9	284.5
P	0.171	9.88×10^{-17}	8.3×10^{-3}	2.60×10^{-18}	2.2×10^{-4}	1.38×10^{-15}
$\Delta H^{\neq}$ (kJ mol^{-1})	182.2	18.2	169.8	0.04	221.2	47.7
$\Delta G^{\neq}$ (kJ mol^{-1})	190.9	199.9	195.1	213.1	280.8	290.4

k, $\Delta S^{\neq}$, $\Delta H^{\neq}$ and $\Delta G^{\neq}$ are calculated at the peak temperature $T_{p(exp)}$.

[27–29]:

$$k = \frac{\chi e k_B T}{h} \exp\left(\frac{\Delta S^{\neq}}{R}\right) \exp\left(-\frac{E}{RT}\right) \qquad (10)$$

where χ is a transmission coefficient which is unity for monomolecular reactions, k_B the Boltzmann constant, h the corresponding Plank constant, $e = 2.7183$ is the Neper number and $\Delta S^{\neq}$ is the change of entropy for the active complex formation from the reagent [20,29,30].

Taking into account the pre-exponential constant A from the Arrhenius Eqs. (2) and (10), the following expression is obtained:

$$A = \frac{\chi e k_B T}{h} \exp\left(\frac{\Delta S^{\neq}}{R}\right) \qquad (11)$$

and $\Delta S^{\neq}$ can be calculated:

$$\Delta S^{\neq} = R\left(\ln A - \ln\frac{\chi e k_B T}{h}\right) \qquad (12)$$

where A is the pre-exponential factor in the Arrhenius equation with values presented in Table 2. Since

$$E = \Delta H^{\neq} + RT \qquad (13)$$

the changes of the enthalpy $\Delta H^{\neq}$ and Gibbs free energy $\Delta G^{\neq}$ for the active complex formation can be calculated using the well known thermodynamical equation:

$$\Delta G^{\neq} = \Delta H^{\neq} - T\Delta S^{\neq} \qquad (14)$$

$\Delta S^{\neq}$, $\Delta H^{\neq}$ and $\Delta G^{\neq}$ were calculated at $T = T_p$ (T_p is the DTG peak temperature), since this temperature characterizes the highest rate of the process and, therefore, is its important parameter.

Based on the analysis and comparison of the values of these parameters, proper conclusion can be made for the kinetics of the pyrolysis of rice husk under the different experimental conditions.

3. Results and discussion

Fig. 1 shows the TG and DTG curves for rice husk treated by all the three methods described.

The TG curves have two plateaus each; the first and smaller one occur around 110 °C and is due to the release of physically adsorbed water. The second one occurs larger and reflects the evaporation of volatile matter and burned carbon. The kinetic studies in this work are devoted to the pyrolysis of the biomass in rice husk. The temperature of the peaks in the DTG curves depends on the heating regime. Therefore, the kinetic parameters characterizing the different processes were expected to be different. The TG data were evaluated using 14 mechanism-based equations (Table 1). The best correlation was obtained with the equation of Ginstling–Brounshtein [31,32]:

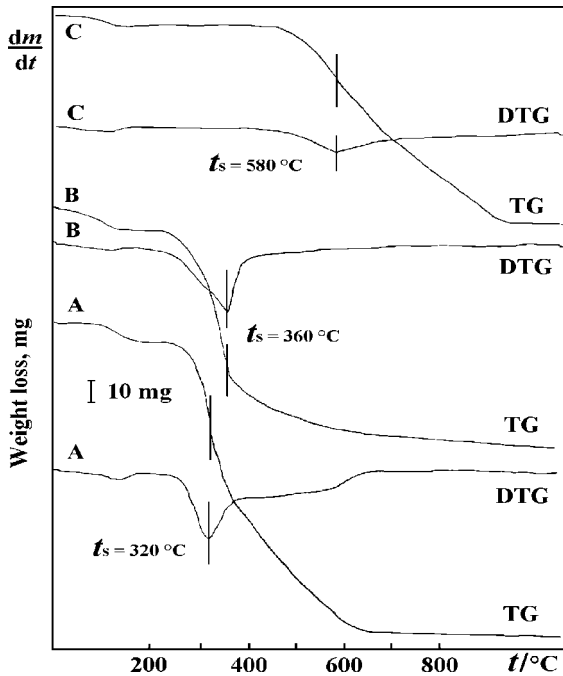$$f(\alpha) = \frac{(2/3)(1-\alpha)^{1/3}}{1 - (1-\alpha)^{1/3}} \qquad (15)$$

Fig. 1. TG and DTG-curves of the samples: (A) degradation in air; (B) pyrolysis in nitrogen flow; and (C) destruction of the pyrolysis product in air.

As it has been discussed in the literature [28,33–35] this equation refers to diffusion controlled reactions starting on the exterior of a spherical particle with radius r_o:

$$g(\alpha) = \left(1 - \frac{2\alpha}{3}\right) - (1-\alpha)^{2/3} = \frac{2kD\tau}{r_o^2} \qquad (16)$$

where D is the coefficient of diffusion.

The substitution of Eq. (16) in Eq. (8) gives:

$$\ln\frac{(1 - 2\alpha/3) - (1-\alpha)^{2/3}}{T^2} = \ln\frac{AR}{qE} - \frac{E}{RT} \qquad (17)$$

Fig. 2 presents graphically the dependence described by Eq. (17) for the three samples studied.

As can be seen, the kinetic curves have two linear regions: the first one at temperatures lower than T_p (peak temperature in DTG curve) is steeper and the second one at higher temperatures has a smaller slope. For detailed study of the mechanisms of both stages, the values of the activation energy E, frequency factor A, change of entropy $\Delta S^{\neq}$, enthalpy $\Delta H^{\neq}$, Gibbs free energy $\Delta G^{\neq}$ were calculated for the formation of the ac-
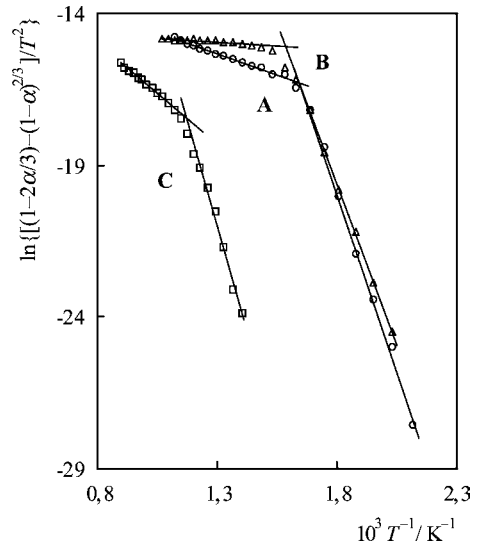

Fig. 2. Ginstling–Brounshtein equation at: (A) degradation in air; (B) pyrolysis in nitrogen flow; and (C) destruction of the pyrolysis product in air.

tive complex from the reagent and $P = \exp(\Delta S^{\neq}/R)$ is the steric factor (Table 2).

Beside the high value of the correlation coefficient of the linear regression analysis R^2, the second criterion used was $T_{p(calc)}$. This temperature was calculated from the cross point between the corresponding straight lines and was compared to the experimentally determined reference temperature $T_{p(exp)}$ which, in turn, corresponds to the peak temperature in the DTG curve. As can be seen from the table, the difference between these two temperatures was less than $4\,^{\circ}C$. It means that the equation of Ginstling–Brounshtein was selected correctly and that a study on the kinetics of pyrolysis of rice husk should take into account the diffusion of volatile products from inside layers of the biomass. The higher values of E observed at $T < T_p$ show that the initial release of volatile products occurs under kinetic-diffusion control while the much lower values of E at $T > T_p$ indicate that pyrolysis takes place under typical diffusion control. The similar values of the activation energy found for the first stages samples A and B show that the release of volatile products during burning in air or pyrolysis in nitrogen medium occurs by similar mechanisms. The difference in E values for the second stage shows that the release of volatile products in nitrogen occurs at

lower activation energy due to their lower content in the sample. At the same time, the oxidative burning of the pyrolysis product (sample C) occurred at much higher activation energies for both stages. This means that the diffusion of the volatile products was much more difficult in sample C because of the hardly deformable Si–O carcass. For monomolecular reactions of decomposition taking place within the solid phase, values of the frequency factor of the order of 10^{14} show that the rotations of the active complex and the reagent do not change during the reaction. At values of ca. 10^{11} the reagent can rotate freely while the active complex can not rotate [28]. The negative values of the change of entropy of the formation of the active complex mean that the active complex can be characterized by a much higher "degree of arrangement" [29]. Besides, higher degree of "arrangement" was observed in the second stage (higher value of $\Delta S^{\neq}$). The significantly lower than unity values of the steric factor P in the second stage give enough grounds to classify this stage as "slow" [29]. For the first stage, however, the values of P are much closer to unity, so the first stage may be considered as "faster" [24].

The diffusion limited process of pyrolysis of rice husk and the correct choice of the equation of Ginstling–Brounshtein was also confirmed by SEM photographs of the samples (Fig. 3).

As can be seen on Fig. 3A, the structure of raw rice husk was globular. It was formed by the relatively stable Si–O carcass and biomass assembled around it. After pyrolysis in air (Fig. 3B), the initial globular structure was preserved. The only difference that can be observed was that the globules were shrinked and densified due to the release of the volatile products. The hard residue was formed of almost pure SiO_2. Obviously, the rate of the pyrolysis process depends strongly on the vapor diffusion rate from the bulk of the spherical globules and the equation of Ginstling–Brounshtein was correctly selected. This process would be more and more diffusion controlled with the increase of the degree of pyrolysis due to the low deformability of the carcass. The structure of the pyrolysis product obtained in nitrogen medium was also globular (Fig. 3C) but, due to the lower percentage of volatile products released, the solid phase contained significantly more carbon. The pyrolysis of this product in air gave a structure similar to the one shown in Fig. 3B. In this case, therefore, the initial
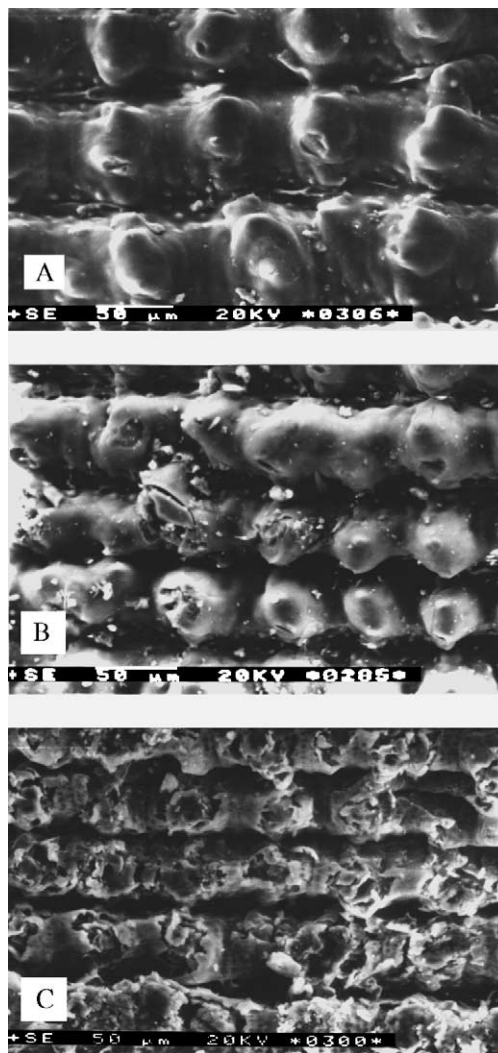

Fig. 3. Secondary electron image of rice husk: (A) raw, before thermal treatment; (B) after thermal degradation in air; and (C) after pyrolysis in nitrogen.

globular structure of the rice husk was also preserved due to the high thermal stability of SiO_2.

As can be seen on Fig. 3C, rice husk pyrolysis in nitrogen medium significantly changes sample texture. The lack of combustion results in denser carbonized mass which, under heating in air (sample C) burned at much higher activation energy.

It may be concluded that the burning of rice husk produces SiO_2 with globular structure and well developed specific area. The pyrolysis in nitrogen medium

gives SiO_2 mixed with carbon. The high thermal stability of the Si–O carcass gives rise to the diffusion controlled pyrolysis process.

Acknowledgements

References

[1] A. Jain, T. Rajeswara Rao, S. Sambi, P. Grover, Biomass Bioenergy 7 (1994) 285.
[2] A. Chakravety, P. Mishra, K. Banerjee, Thermochim. Acta 94 (1985) 267.
[3] A. Sharma, T.R. Rao, Bioresource Technol. 67 (1999) 53.
[4] D.M. Ibrahim, M. Helmy, Thermochim. Acta 45 (1981) 79.
[5] M. Devan, in: Proceedings of the National Workshop on Rice Husk for Energy, Vigian Bhawan, New Delhi, 1982, p. 35.
[6] H.D. Banerjee, H.N. Acharya, S.K. Duta, Indian J. Technol. 18 (1980) 84.
[7] A. Karera, S. Nargis, S. Patel, M. Patel, J. Scient. Ind. Res. 45 (10) (1986) 441.
[8] M. Patel, A. Karera, P. Prasanna, J. Mater. Sci. 22 (1987) 2457.
[9] R.V. Krishnarao, M.M. Godkhindi, P.G.I. Mukunda, M. Chakraborty, J. Am. Ceram. Soc. 74 (11) (1991) 2869.
[10] A.S. Vlasov, A.I. Zaharov, O.A. Sarkisyan, N.A. Lukashev, Ogneupory 10 (1991) 15.
[11] L.A. Lyubchev, I.G. Markovska, in: Proceedings of the International Symposium "Ecology 93", 9–11 September 1993, Bourgas, Bulgaria, p. 32.
[12] H.D. Banerjee, S. Sen, H.N. Acharya, Mater. Sci. Eng. 52 (1982) 173.
[13] M.A. Hamad, J. Chem. Tech. Biotechnol. 31 (1981) 624.
[14] A.K. Roberts, Combust. Flame 14 (1970) 261.
[15] A.M. Kanury, Combust. Flame 18 (1972) 75.
[16] C.A. Koufopanos, G. Maschio, G. Lucchesi, Can. J. Chem. Eng. 67 (1989) 75.
[17] S. Gaur, T.B. Reed, Biomass Bioenergy 7 (1994) 61.
[18] A.W. Coats, J.P. Redfern, Nature 201 (1964) 69.
[19] A.W. Coats, J.P. Redfern, J. Polym. Sci., Part B 3 (1965) 917.
[20] V. Indira, G. Parameswaran, J. Therm. Anal. 32 (1987) 1151.
[21] P.V. Khadikar, J. Therm. Anal. 32 (1987) 737.
[22] N.Sh. Petro, B.S. Girgis, J. Therm. Anal. 34 (1988) 37.
[23] K.N. Ninan, J. Therm. Anal. 35 (1989) 1267.
[24] J.J.M. Orfao, F.G. Martins, Thermochim. Acta 390 (2002) 195.
[25] C.L. Albano, R. Siamanna, T. Aquino, J. Martinez, in: Proceedings of the European Congress on Computational Methods in Applied Science and Engineering, Barcelona, 2000.
[26] V. Mamleev, S. Borbigot, M. Le Bras, S. Daquese, J. Sestak, Phys. Chem. Chem. Phys. 2 (2000) 4708.
[27] A.M. Urzhenko, A.V. Usherov-Marshak, Neorg. mater. 10 (5) (1974) 888.
[28] J. Sestak, Thermochemical Properties of Solids, Academica, Prague, 1984.
[29] D.V. Sokolskii, V.A. Druz, Vvedenie v teoriy geterogenogo kataliza, Vischaya Shkola, Moscow, 1981.
[30] L.H. McAmish, F.J. Jhonston, J. Inorg. Nucl. Chem. 38 (1976) 537.
[31] A.M. Ginstling, L.I. Brounshtein, Zh. Prikl. Khim. 23 (12) (1950) 1247.
[32] B.I. Brounshtein, A.M. Ginstling, Zh. Prikl. Khim. 29 (12) (1956) 1870.
[33] E.A. Giess, J. Am. Ceram. Soc. 46 (8) (1963) 374.
[34] I. Horvath, P. Komadel, L. Galikova, Silikaty (Prague) 28 (1984) 317.
[35] Yu.D. Tretyakov, H. Lepis, Khimiya i tekhnologiya tverdofaznikh materialov, Mosk. Universitet, Moscow, 1985.